Journal of Alloys and Compounds 560 (2013) 215–222

Contents lists available at SciVerse ScienceDirect

Journal of Alloys and Compounds

journal homepage: www.elsevier.com/locate/jalcom

Electronic structure and vibrational properties in cobalt-based full-Heusler compounds: A first principle study of Co_2MnX (X = Si, Ge, Al, Ga)

A. Candan [a], G. Uğur [b,*], Z. Charifi [c,*], H. Baaziz [c], M.R. Ellialtıoğlu [d]

[a] Central Research and Practice Laboratory (AHILAB), Ahi Evran University, 40100 Bağbaşı-Kırşehir, Turkey
[b] Department of Physics, Faculty of Science, Gazi University, 06500 Ankara, Turkey
[c] Department of Physics, Faculty of Science, University of M'sila, 28000 M'sila, Algeria
[d] Department of Physics Engineering, Faculty of Engineering, Hacettepe University, 06800 Ankara, Turkey

ARTICLE INFO

Article history:
Received 20 December 2012
Received in revised form 21 January 2013
Accepted 23 January 2013
Available online 13 February 2013

Keywords:
Half metal
Heusler alloy
Density functional theory
Elastic constants
Phonon properties
Density of states

ABSTRACT

First-principles self-consistent pseudopotential plane wave calculations based on density functional theory were performed in order to study magnetic moments, density of states and half-metallicity of $L2_1$ type full Heusler alloys with formula Co_2MnX (X = Si, Ge, Al, Ga). Half-metallicity in terms of total spin-moments was discussed since perfect half-metals show Slater–Pauling (SP) behavior. The effects of the atomic number on the lattice constants, the bulk moduli and the Curie temperatures were shown. The magnetic moments were calculated, while slight deviations of about 0.06–0.16 μ_B were found for Co_2MnAl and Co_2MnGa, the Co_2MnSi and Co_2MnGe have been found to be half metals. Mechanical stability of these compounds has been analyzed in terms of their elastic constants. The size of the gap in the minority states and the position of E_F inside the gap was also discussed as it is an important factor for the application of half-metallic ferromagnetic alloys. Finally, phonon dispersion curves and the density of states were calculated by employing the density-functional perturbation theory and discussed.

1. Introduction

Half-metallic ferromagnetic alloys (HMFs) are presently under intense investigation [1–6]. They show mixture properties of metal and semiconductor. They are fully spin polarized around Fermi energy level (E_F): while one spin projection has metallic character at E_F, the other spin projection demonstrates semiconductor-like character [7]. Recently, HMFs have attracted attention since they show great potential for spintronics such as tunneling magnetoresistance (TMR) and giant magnetoresistance (GMR) elements [1] and also for electro-mechanical [8] applications.

Full-Heusler alloys, such as Co_2MnSi, Co_2MnGe, gained a particular interest and became most widely studied in this field due to their high Curie temperatures, a requirement for integration into devices [9]. They have been predicted from first-principles to be half metallic and potential candidates for spintronic applications. However, spin polarizations of only 50–60% were experimentally obtained for these compounds, a decrease attributed to defects in the Mn and Co sublattices [10–13] and to thermally excited magnons [14]. One of the most attractive features of Heusler compounds is the possibility to tune their magnetic properties, such as M_s [15,16], T_c [17], and Fermi level position [9,18], using the chemical handle provided by the number of valence electrons Z_t. The Heusler compounds are well known to be systematized by the number of valence electrons Z_t. Striking examples are the magnetic moment described by the Slater–Pauling rule (SP rule) [2,19,20] or the Curie temperature T_c [17], which are both generally proportional to Z_t. A second advantage of Heusler alloys for realistic applications is their structural similarity to the zinc-blende structure, adopted by binary semiconductors widely used in industry (such as GaAs and ZnS).

Among the predicted half-metallic ferromagnets, the Co_2MnX (with X = Si, Ge, Ga, Al) full-Heusler family with $L2_1$ structure is regarded as one of the most promising candidates for a high efficiency TMR device [21,22] because of its ideal 100% spin polarization for (Co_2MnSi and Co_2MnGe) at the Fermi level, a good structural matching with main stream semiconductors (in terms of lattice constants and crystal structure) and very high Curie temperatures [1,11] about 900 K, while for the other compounds the Curie temperature is near room temperature. Recently, it has been found that several Co_2MZ Heusler alloys had high spin polarizations more than 85% [5,14], much higher than 3d transition metals and their alloys, which typically have spin polarizations of about 45% or lower [23,24].

Generally, the full-Heusler alloys show a Slater–Pauling behavior and the total spin-magnetic moment per unit cell (M_t) scales with the total number of valence electrons (Z_t) following the rule:

* Corresponding authors. Tel.: +90 3122121255; fax: +90 3122122279 (G. Uğur), tel./fax: +213 35556453 (Z. Charifi).
E-mail addresses: gokay@gazi.edu.tr (G. Uğur), charifizoulikha@gmail.com (Z. Charifi).

0925-8388/$ - see front matter © 2013 Elsevier B.V. All rights reserved.
http://dx.doi.org/10.1016/j.jallcom.2013.01.102

$M_t = Z_t - 24$. As a result half-metallic ferromagnets, such as the Heusler compounds with formula X_2YZ, are expected to show an integer value for the spin magnetic moment. This later quantity is an important characteristic property for these systems in stoichiometric compositions. The small deviations from integer magnetic moment would lead to significant disruptions in half-metallic character by non-zero electronic density of states for minority spins around Fermi level [25]. In contrast to experiments, calculations give noninteger values in certain cases where the compounds are based on Co which is our case for Co_2MnGa and Co_2MnAl. Webster studied the chemical and magnetic structures of the alloys Co_2MnX (X = Al, Ga, Si, Ge, Sn) and reported [26] that the alloys with X = Si, Ge and Sn had net moments of approximately 5.1 μ_B per molecule with individual moments of 0.75 μ_B and 3.6 μ_B on Co and Mn sites, respectively, and that the alloys containing Al or Ga have net moments of approximately 4.0 μ_B per molecule and correspondingly smaller moments on both Co and Mn sites [26]. In addition, for Co_2MnSi, a Curie temperature of T_c = 985 K and a total magnetic moment of about 5 μ_B [21,27,28] have been measured.

The knowledge of the basic magnetic, electronic and vibrational properties of these materials, is required in order to fully exploit these promising materials, to design new generation spin-dependent devices, to understand their underlying electronic structure and to establish structure–property relationships. In the present work, by means of a DFT approach we examined the series of Heusler alloys Co_2MnX (with X = Si, Ge, Al, Ga) assuming they crystallize in the typical $L2_1$ structure. We find that, while there have been a number of works focused on the electronic and magnetic properties of these alloys, there has been little effort, to the best of our knowledge, to investigate these system in term of their elastic and phonon properties. We derived magnetic and electronic properties as well as vibrational and elastic properties for all of these compounds, and we also investigated the influence of X atomic number on the electronic structure.

In Section 2, we report some details about the crystal structure and the numerical values. We concentrate on the equilibrium lattice constant, bulk modulus and magnetic moments in Section 3.1. We focus on the elastic properties in Section 3.2 and discuss the electronic properties in terms of band structures and density of states, and we analyze the vibrational properties in Section 3.3, and finally, we draw conclusions in Section 4.

2. The crystal structure and calculational details

Heusler compounds are good candidates for spintronic materials since they combine high Curie temperatures and coherent growth on top of semiconductors [2,29]. $-X_2YZ$ Heusler compounds crystallize in the $L2_1$ structure (see Fig. 1)., they consist of four fcc sublattices with each one occupied by a single chemical element at A (0,0,0), C(1/2,1/2,1/2), B(1/4,1/4,1/4), and D(3/4,3/4,3/4) positions. They belong to the Fm3m space group. In general, X and Y atoms are transition metals and Z is a main group element. In the compound Co_2MnX (with X = Si, Ge, Al, Ga) each Mn or sp atom has eight Co atoms as first neighbors sitting in an octahedral symmetry position, while each Co has four Mn and four sp atoms as first neighbors and thus the symmetry of the crystal is reduced to the tetrahedral one.

The first-principles studies of the Co_2MnX (with X = Si, Ge, Al, Ga) Heusler compounds are performed by employing the self-consistent ultrasoft pseudopotential method [30] based on the density functional theory. The exchange-correlation potential were described within the generalized gradient approximation (GGA) of Perdew–Burke–Ernzerhof (PBE) [31,32], incorporated into the quantum-Espresso code [33]. Nonmagnetic as well as ferromagnetic orderings were considered. The energy cutoff for the expansion of the eigenfunctions was set to 40 Ry. The electronic charge density was evaluated up to the kinetic energy cut-off of 400 Ry. A grid of (10 × 10 × 10) k-points generated was symmetry reduced and used to sample the irreducible wedge of the first Brillouin zone. Integration up to the Fermi surface was performed using the smearing technique [34] with smearing parameter σ = 0.02 Ry. When exploring the electronic structure, a finer grid (35 × 35 × 35) was chosen to generate a high quality charge density. With these choices, the total energy is converged to 1 mRy per atom. Having obtained self-consistent solutions of Kohn–Sham equations, the lattice-dynamical properties were calculated within the framework of the self-consistent density functional perturbation theory [35]. To obtain complete phonon dispersions and density of states, eight dynamical matrices were calculated on a (4 × 4 × 4) q-point mesh. The dynamical matrices at arbitrary wave vectors were evaluated using Fourier deconvolution on this mesh. The ground state of each compound was found by minimizing the total energy as a function of the lattice parameters.

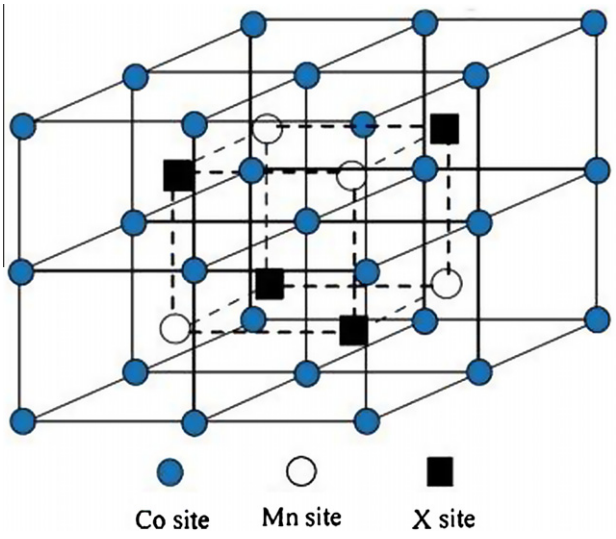

Fig. 1. The $L2_1$ structure of Heusler alloys Co_2MnX (X = Si, Ge, Al, Ga).

3. Results and discussion

3.1. ground-state properties

We performed calculations of the electronic structures of four Co-based Heusler alloys with the generic formula Co_2MnX (with X = Si, Ge, Al, Ga). It was found that the ferromagnetic spin-polarized configuration had a lower minimum total energy than that found in the paramagnetic non spin polarized case. The same behavior was observed in a previous work reported in ref. [36] that Co_2MnZ alloys, where Z is Si, Al, Ga, Sn, Sb, were ferromagnetic and had relatively large Curie temperatures compared to most other Mn-based Heusler alloys with $L2_1$ structure. The volume optimization was performed using several lattice constants near the experimental ones. The calculated total energies within GGA as functions of the volume were fitted to Murnaghan's equation of state to obtain the ground-state properties [37].

In Table 1, we report our calculated equilibrium lattice constant, along with bulk modulus and the total magnetic moment, the density of states at the Fermi level (E_F), compared with the available experimental and theoretical data [11,26,38–42]. The bulk

Table 1
Calculated lattice constant a, bulk modulus B and its pressure derivative B', the total magnetic moment and the density of states at Fermi energy $N(E_F)$ for Co_2MnX (with X = Si, Ge, Al, Ga) full-Heusler, compared with the available experimental and theoretical data.

Material	Reference	a_0 (Å)	B (GPa)	B'	M_t (μ_B)	$N(E_F)$ (states/eV cell)	
						$N(\uparrow, E_F)$	$N(\downarrow, E_F)$
Co_2MnSi	This work	5,633	212.8	4.680	5.00	1.17	0
	Exp [26]	5.654	–	–	5.07		
	Theoretical [11]	5.634	226	–	5.00		
	Theoretical [38]	5.643	–	–	5.00		
	Theoretical [39]	5.523	–	–	5.06		
	Theoretical [40]	5.639	214	4.674	5.00		
	[45]	–	–	–	–	0.31	
Co_2MnGe	This work	5.753	191.4	4.54	5.01	1.33	0
	Exp [26]	5.743	–	–	5.11		
	Theoretical [11]	5.734	188	–	5.00		
	Theoretical [39]	5.618	–	–	4.99		
	Theoretical [42]	5.729	–	–	4.99		
Co_2MnAl	This work	5.707	181.3	4.43	4.06	1.16	0.244
	Exp [26]	5.756	–	–	4.01		
	Theoretical [38]	5.695	–	–	4.04		
	Theoretical [39]	5.586	–	–	4.03		
Co_2MnGa	This work	5.724	186.7	–	4.16	1.7	0.381
	Exp [26]	5.770	–	–	4.05		
	Theoretical [39]	5.586	–	–	4.08		
	Theoretical [41]	5.724	199	–	4.08		
	Theoretical [42]	5.710	–	–	–		

modulus increases by 2.3% when we replace Al by Ga, however, it decreases when we substitute Ge for Si by about 11.18%. We mention that the bulk modulus of Co_2MnSi is the largest one of about 212.8 GPa, and as a result, it is predicted to be the hardest in the studied series.

Another important point is that in Heusler materials like the ones studied here the total spin moment should be an integer number since both the total number of valence electrons as well as the number of occupied minority states are integers. However our results in Table 1 do not give integer numbers for the total moments, but slight deviations of about 0.06–0.16 μ_B were found for Co_2MnAl and Co_2MnGa. As a matter of fact their total spin moments were found to be 4.06 μ_B and 4.16 μ_B, respectively, compared to the ideal 4 μ_B predicted by the SP rule while those of the Si and Ge-based alloys are exactly 5 μ_B as predicted by the SP rule and measured in previous works [21,27,28]. The total spin moment for Co_2MnGe, was found to be 5.01 μ_B, with a minute deviation that is possibly due to inaccuracies associated with the numerical integration. The magnetic moments are mainly due to the Mn atoms while the magnetic transition metal Co atoms also contribute to additional magnetic moments; this observation is consistent with a previous work reported in [14]. The Co atoms are ferromagnetically coupled to the Mn spin moments and they possess a spin moment that varies from 0.7 to 1.0 μ_B, while the sp atom has a very small negative moment which is an order of magnitude smaller than the Co moment. The replacement of Al or Ga by Si or Ge in Co-based alloys leads to substantial increase of magnetic moment from 4 to 5 whereas the replacement of Al by Ga or Si by Ge does not change the value of total magnetic moment.

The Curie temperatures T_c for Co_2MnX (with X = Si, Ge, Al, Ga) were estimated according to the model presented in Ref. [15] by applying the linear relation $T_c = 23 + 181M_t$. The values found are 928, 930, 758 and 776 K for Co_2MnSi, Co_2MnGe, Co_2MnAl and Co_2MnGa, respectively. The Co_2MnGe and Co_2MnSi compounds are of special interest, because of their rather large T_c values, making them interesting for technological applications. It is clearly seen that the Curie temperature increases as the X atomic number increases with the same valence number Z_t, in addition, it is noted that the calculated T_c value of Co_2MnSi is less than that found experimentally, but in agreement with the results of others as reported in [21,27,28].

3.2. Elastic properties and mechanical stability

The elastic constants C_{ij} contain some of the more important information which can be obtained from ground state total energy calculations. The C_{ij} can be used to check the phase stability of the studied compounds, and provide an estimation of the strength and indirectly the melting temperature [43]. To obtain the elastic constants of these compounds with cubic structure we have used numerical first principles calculation by computing the components of the stress tensor e for small strains, using the method reported in ref [44]. It is well known that a cubic crystal has only three independent elastic constants.

The theoretical elastic constants are calculated from the energy variation by applying small strains to the equilibrium lattice configuration. The elastic energy change under strain is given by:

$$\frac{\Delta E}{V} = \frac{V}{2}\sum_{i=1}^{6}\sum_{j=1}^{6} C_{ij} e_i e_j \tag{1}$$

where V is the volume of the undistorted lattice cell, ΔE is the energy increment by the strain with vector $e = (e_1, e_2, e_3, e_4, e_5, e_6)$, and C is the matrix of elastic constants. The primitive vectors a_i ($i = 1, \ldots, 3$) of crystals are transformed to the new vectors under the strain by

$$\begin{pmatrix} a_1' \\ a_2' \\ a_3' \end{pmatrix} = \begin{pmatrix} a_1 \\ a_2 \\ a_3 \end{pmatrix} \cdot (I + \varepsilon) \tag{2}$$

where ε is the strain tensor. It relates to the strain vector e by

$$\varepsilon = \begin{pmatrix} e_1 & e_6/2 & e_5/2 \\ e_6/2 & e_2 & e_4/2 \\ e_5/2 & e_4/2 & e_3 \end{pmatrix} \tag{3}$$

For the strain under hydrostatic pressure $e = (\delta, \delta, \delta, 0, 0, 0)$, which transforms the total energy change into:

$$\frac{\Delta E}{V} = \frac{9}{2} B\delta^2 \quad (4)$$

where B is the bulk modulus with $B = (C_{11} + 2C_{12})/3$.

Under the volume-conserving monoclinic strain $e = (0, 0, \delta^2/(4 - \delta^2), 0, 0, \delta)$, the total energy is changed from its initial value as follows:

$$\frac{\Delta E}{V} = \frac{1}{2} C_{44}\delta^2 + O(\delta^4) \quad (5)$$

Finally, for the last type of deformation, we used the volume-conserving rhombohedral strain tensor given by $e = (0, 0, (1 + \delta)^{-2} - 1, 0, 0, \delta)$ which transforms the total energy to:

$$\frac{\Delta E}{V} = 6C'\delta^2 + O(\delta^3) \quad (6)$$

where C' is defined by $C' = (C_{11} - C_{12})/2$.

In this study, we calculated 21 sets of $\frac{\Delta E}{V}$ by varying δ from -0.02 to 0.02 in steps of 0.002. These data are fitted by a quadratic polynomial and then the relevant elastic constant is obtained from the coefficient of the corresponding quadratic term in Eqs. (4)–(6). They are listed in Table 2, together with the data available from experimental and other calculations for comparison [41,45]. Our estimated elastic constants of Co_2MnSi are in excellent agreements with those calculated with the same method incorporated in VASP code by Chen et al [45]. The elastic constants increase as we replace Ge by Si, but they decrease when we replace Ga by Al in Co_2MnX (with X = Si, Ge, Al, Ga) Heusler alloys except for C_{44}.

Mechanical stability of these compounds has been analyzed in terms of their elastic constants. For cubic crystals, the conditions for mechanical stability are given by [46]:

$$C_{44} > 0, \quad (C_{11} - C_{12})/2 > 0 \quad \text{and} \quad B = (C_{11} + 2C_{12})/3 > 0 \quad (7)$$

From Table 2, we see that these criteria are met, so we conclude that all the compounds in the $L2_1$ phase are stable.

3.3. Electronic and vibrational properties

Spin-polarized band structure calculations for the Co_2MnX (with X = Si, Ge, Al, Ga) Heusler alloys have been investigated. The results for the electronic spectra are in good agreement with the existing calculations reported in the literature [11,16,36,47]. Fig. 2 displays the band structure of Co_2MnX (with X = Si, Ge, Al, Ga). The majority spin band (Fig. 2a, c, e, and g) exhibits metallic character, i.e. the valence band is partially filled, providing conducting electrons at the Fermi level E_F. The picture is quite different for the minority spin band (Fig. 2b and d), where E_F is seen to lie within the band gap, which is reminiscent of a semiconductor. We conclude that the Heusler compounds Co_2MnSi and Co_2MnGe show true half-metallicity.

For pure Co_2MnAl and Co_2MnGa, both the majority-spin and minority-spin bands show intersections with the E_F (see Fig. 2e–h), showing metallic character for both spin channels. These alloys present a region of very small minority density of states instead of a real gap; so called pseudogap. So, we can conclude that the full Heusler alloys Co_2MnAl and Co_2MnGa show traditional ferromagnetism-false half-metallicity under normal conditions, they are nearly half-metallic. Same result was found by Kübler et al. [36] that the minority spin densities at the Fermi energy nearly vanish for Co_2MnAl and Co_2MnSn. The polarizations at the Fermi level, $P(E_F)$ are 0.65 and 0.63 for Co_2MnAl and Co_2MnGa, respectively, indicating ferromagnetic character. Generally speaking, one can conclude that there is a close relationship between the magnetic moment and the (HMF) character. The appearance of the gap in the minority density of states constrains the number of minority electrons to be integer. However, an integer value of the magnetic moment may not automatically result in a real gap in the minority or majority density of states.

An important factor for the application of the HMFs is the size of the gap in the minority states and the position of E_F inside of the gap is also of interest. Small gaps may be easily destroyed by temperature effects. The half-metallicity may also be easily destroyed if E_F is located close to the band edges, either of the minority valence or conduction bands [48]. Both Co_2MnAl and Co_2MnGa have E_F outside of the minority band gap. In the case of Co_2MnGe, E_F is approximately close to the top of the valence band, whereas for Co_2MnSi, it is inside the gap as shown in Fig. 2b, d, f, and g. At the same time the Fermi energy moves from near the middle of the minority valence states gap (Co2MnSi) towards the top of the minority valence band (Co2MnGe) then it intersects the valence band of Co_2MnAl and Co_2MnGa compounds. According to Fig. 2b and d the width of the band gap has values in the range of 0.59 to 0.77 eV for Co_2MnGe and Co_2MnSi respectively. The upper valence bands shift towards the Fermi level (EF) when the atomic number increases and they cross E_F in Co_2MnAl and Co_2MnGa Heusler alloys causing a negative spin flip gap. The spin-flip's values of Co_2MnX Heusler alloys are 0.31, 0.02, -0.24 and -0.49 eV for X being Si, Ge, Al and Ga, respectively. We conclude that the energy gap and the spin gap of Co_2MnGe and Co_2MnSi increase as the X atomic number decreases.

For a better understanding of the electronic states, the spin-dependent partial DOS of Co and Mn 3d states are depicted in Fig. 3. While the X sp orbitals contribute to the bonding states far below the Fermi level, the electronic states around E_F is dominated by the 3d states of the Mn and Co atoms, and the majority spin states are nearly fully occupied. The DOS curves for the minority spins exhibit two peaks above the Fermi level which are due to both Mn and Co 3d contributions. For minority spin orbitals, we observe that the minority d states of Mn are generally shifted to higher energies compared to the d orbitals of Co due to stronger exchange splitting at the Mn atoms. Hence the two types of d orbitals only partially mix with each other. As evidenced by the integer total magnetic moment of 5 μ_B per unit cell of Co_2MnSi. Most of the intensity of these unoccupied states comes from Mn d orbitals. In contrast, the states directly above and below the minority spin gap were found to have mostly Co d character.

Table 2
Calculated elastic constants C_{ij} (GPa) and the curie temperature, for Co2MnX (with X = Si, Ge, Ga, Al) full-Heusler alloys compared with the available theoretical data.

Material	Reference	B (GPa)	C_{11} (GPa)	C_{12} (GPa)	C_{44} (GPa)	T_c (K)
Co_2MnSi	This study	213.55	311.16	164.75	153.26	928
	Theoretical [45]	221	316	174	143	
	[21,27,28]					985
Co_2MnGe	This study	192.69	270.53	153.77	126.55	930
Co_2MnAl	This study	184.02	264.03	144.02	155.91	758
Co_2MnGa	This study	184.21	241.44	155.60	132.80	776
	Theoretical [41]	–	–	–	175	

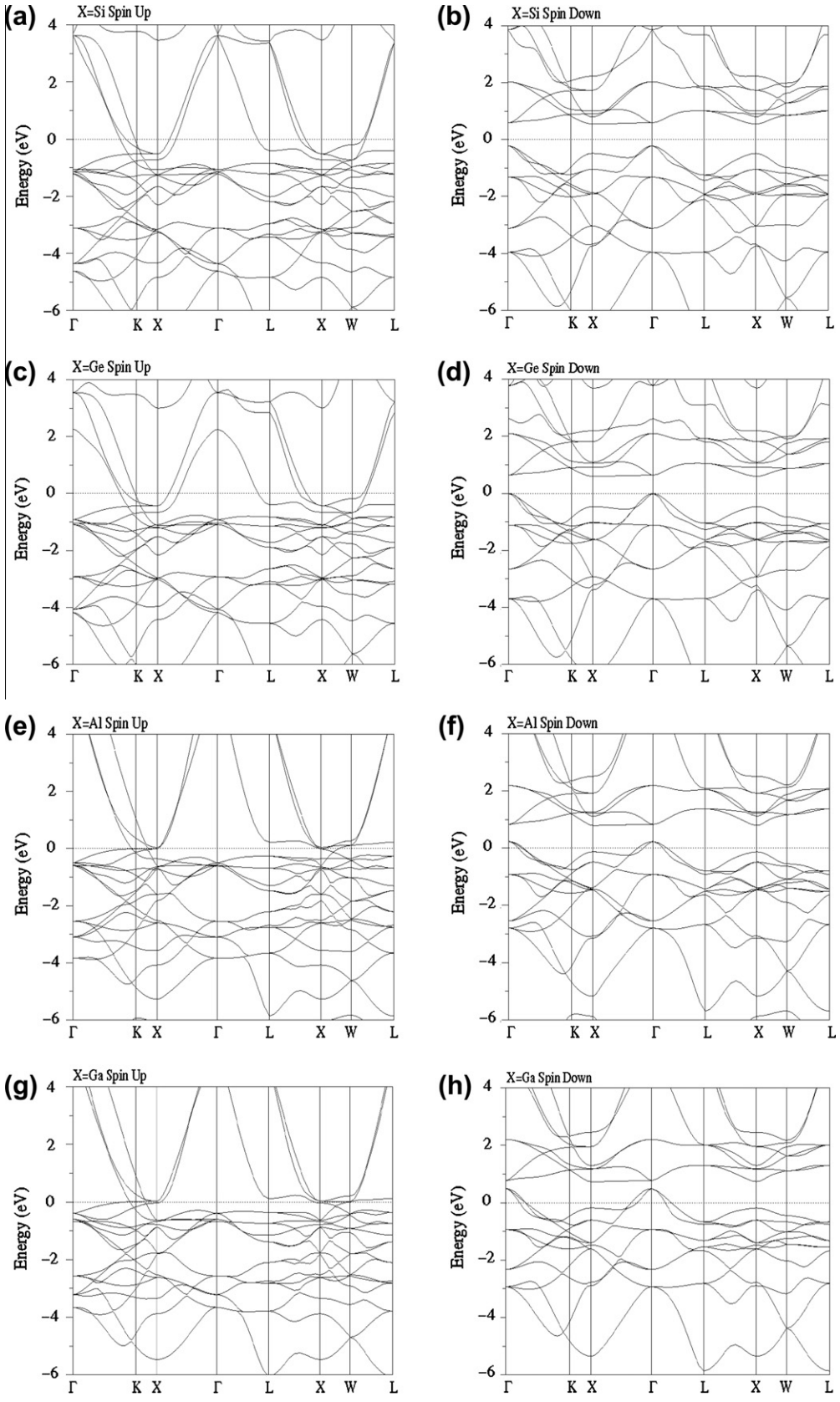

Fig. 2. Calculated electronic band structure of Co_2MnX (X = Si, Ge, Al, Ga) Heusler alloys.

Fig. 4 shows a comparison between the density of states of Co_2MnGa and of Co_2MnAl on one hand and Co_2MnSi and Co_2MnGe on the other hand. The Fermi levels are shown by the dashed vertical lines in both DOS plots. The overall features are similar in compounds with same Z_t, however, it is evident that there are some differences in the DOS of these Heusler alloys due to both

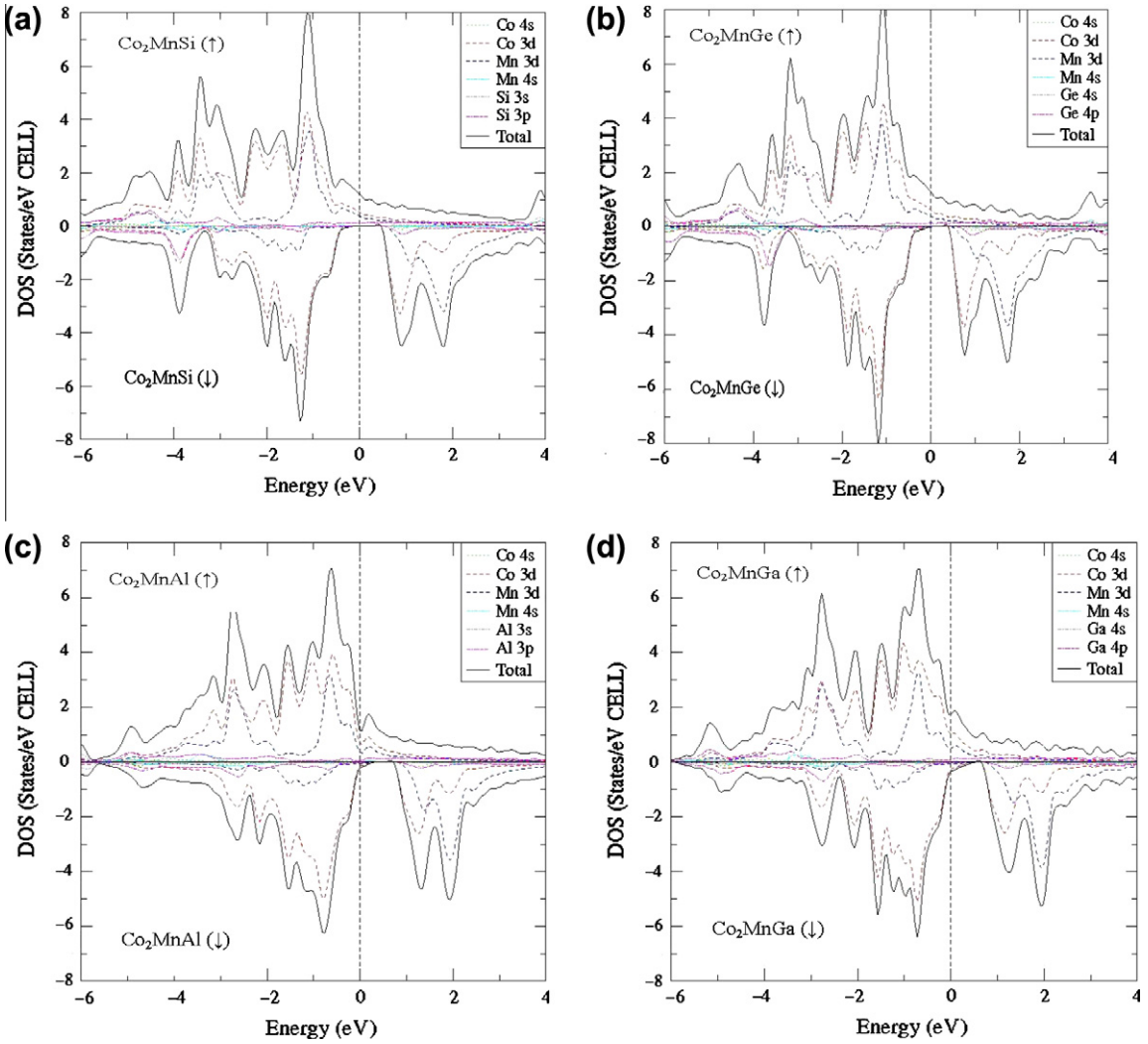

Fig. 3. The total and partial DOS of Co_2MnX (X = Si, Ge, Al, Ga) Heusler alloys.

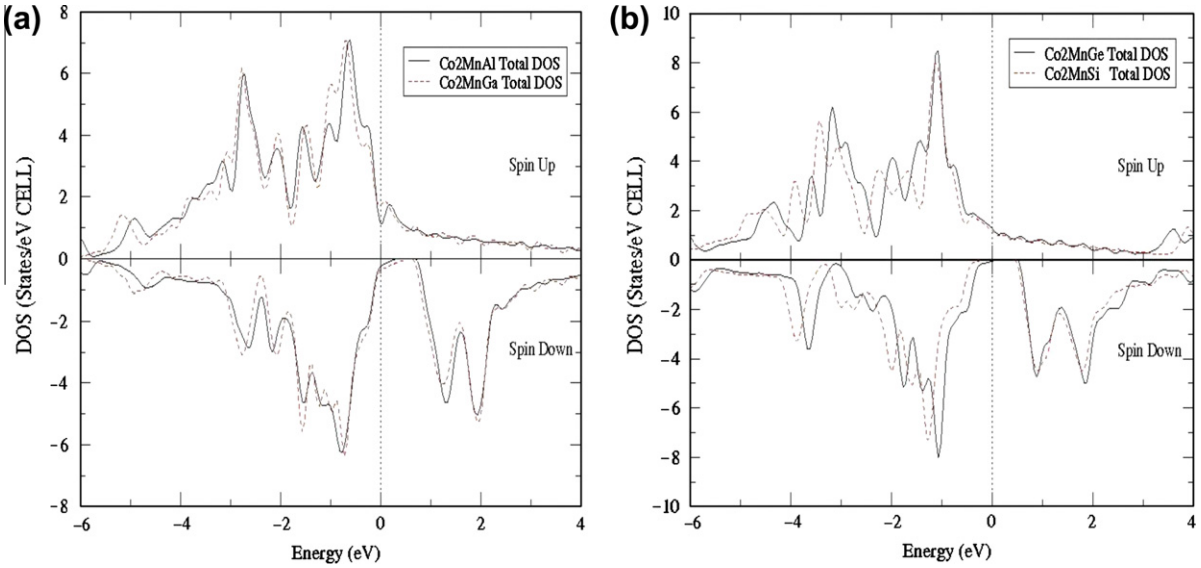

Fig. 4. The effect of atomic number *X* on total DOS of (a) Co_2MnSi and Co_2MnGe and (b) Co_2MnAl and Co_2MnGa Heusler alloys.

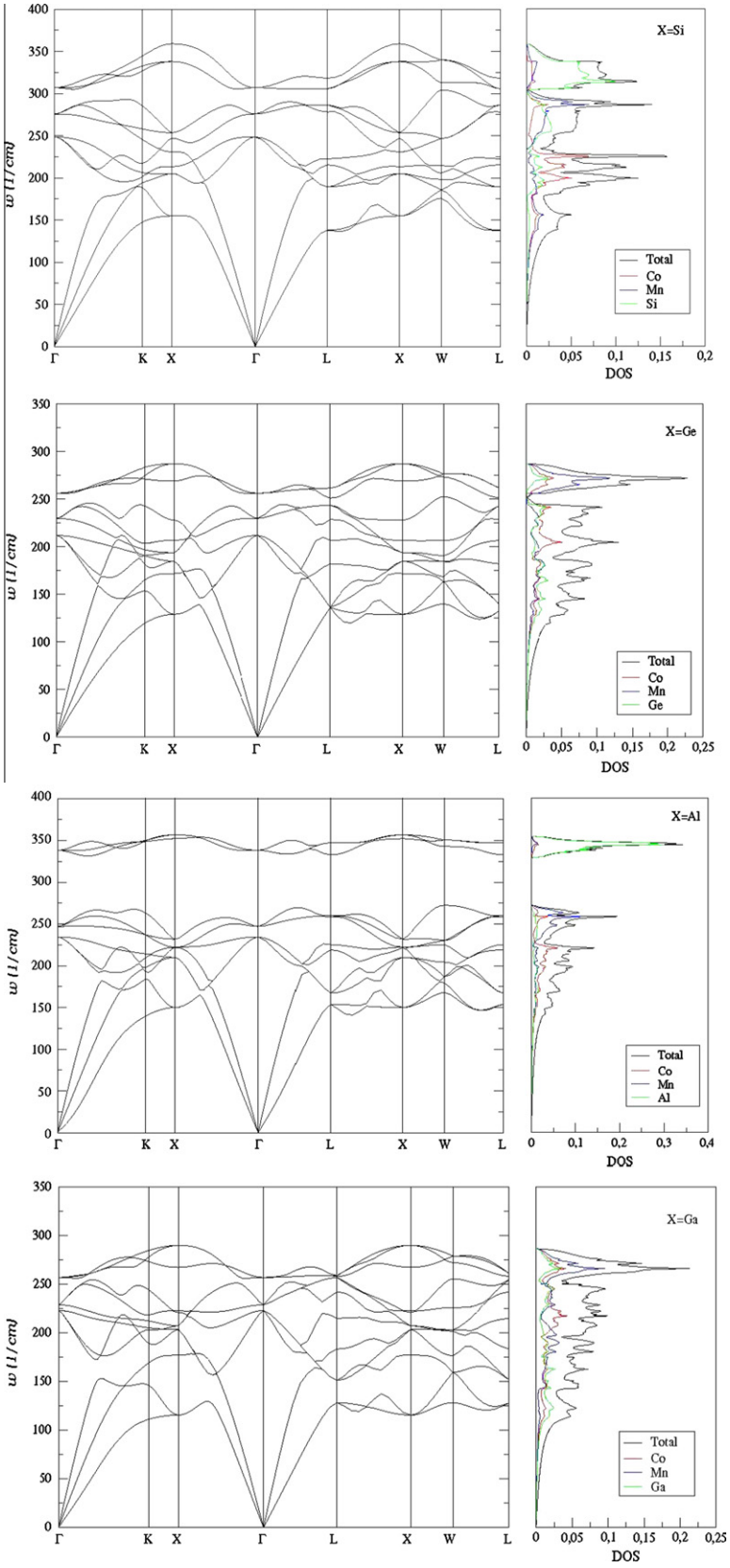

Fig. 5. Calculated phonon dispersion curves and phonon DOS for Co_2MnX (X = Si, Ge, Al, Ga) Heusler alloys along several lines of high symmetry in the Brillouin zone.

the presence of different *X* atoms and different volumes. The substitution of the *X* atom alters slightly both the position of E_F and the band gap. The dependence of the electronic structures of the Co_2MnX alloys on the chemical nature of the isoelectronic *X* atom has been clearly seen in Fig. 4a and b. All peaks below the Fermi level move to higher energies with increasing lattice parameters

because of the enlarged atomic radii. Because the changes in peak positions upon exchanging the X element is proportional to the change in the lattice parameter, the replacement of Si by Ge has bigger consequences than the replacement of Al by Ga.

Our results for the phonon dispersion along the symmetry lines, together with the corresponding partial and total density-of-states, are presented in Fig. 5. Since the unit cell contains four atoms, there are 12 vibrational phonon modes for any chosen q point. However, transverse branches are degenerate along certain high-symmetry directions. The absence of any imaginary or negative vibrational mode confirms its dynamical stability. The obtained optical mode frequencies at the zone center (Γ-point) are 248 cm^{-1}, 275 cm^{-1} and 307 cm^{-1} for Co_2MnSi, 212 cm^{-1}, 229 cm^{-1} and 256 cm^{-1} for Co_2MnGe, 234 cm^{-1}, 246 cm^{-1} and 338 cm^{-1} for Co_2MnAl, and 223 cm^{-1}, 228 cm^{-1} and 257 cm^{-1} for Co_2MnGa. The frequencies at the Γ-point for Co_2MnGa and Co_2MnGe are in good agreement with previous first principles calculations of Zayak et al. [42]. The dispersion of the acoustic branches along Γ–X symmetry directions for Co_2MnGa and Co_2MnGe also agree well with the theoretical results [42]. The partial phonon density of states shows that the Mn and X (Si, Ge, Al, Ga) atoms mainly contribute to the high frequency vibrations because of their lighter atomic masses, while the heavier Co atom dominates the low frequency vibrations. There is significant band gap (59.08 cm^{-1}) between the optical and optical phonon modes for Co_2MnAl. Co_2MnSi shows relatively small gap (0.82 cm^{-1}) between optical and optical modes.

4. Conclusion

In the present work, we performed the first-principle calculations of the total energy, total and partial density of states, magnetic moments for a series of Co containing bulk Heusler alloys Co_2MnX (with X = Si, Ge, Al, Ga). The electronic structure calculations were performed using pseudopotentials. The exchange-correlation functional was evaluated within the GGA, using the Perdew–Burke–Ernzerhof parametrization. We found that the lattice constant increases as we increase the X atomic number by 2.1% when substituting Ge for Si and by 0.3% upon substituting Ga for Al. On the other hand the bulk modulus increases by 2.3% when we replace Al by Ga however it decreases when we substitute Ge for Si by about 11.18%. The full Heusler alloys Co_2MnAl and Co_2MnGa have total spin moments 4.06 μ_B and 4.16 μ_B, respectively, slightly larger than the ideal 4 μ_B predicted by the Slater–Pauling rule, while those of the Si and Ge-based alloys are exactly 5 μ_B. The values of the Curie temperature found are 928, 930, 758 and 776 K for Co_2MnSi, Co_2MnGe, Co_2MnAl and Co_2MnGa, respectively. It is clearly seen that the Curie temperature increases as the X atomic number increases with the same valence number Z_t. The elastic constants C_{ij} are estimated from the energy variation as a function of stress. Elastically, all the compounds have been found to be stable in the $L2_1$ phase. All Co_2MnX compounds exhibit a gap in the minority states band and are with the exception of Co_2MnAl and Co_2MnGa, clearly half-metallic ferromagnets. The substitution of the X atom alters slightly both the position of E_F and the band gap. The compounds Co_2MnAl and Co_2MnGa are very close to half metallicity. The phonon frequencies and the phonon densities of states in the $L2_1$ phase in several lines of high symmetry of the Brillouin zone, were obtained and discussed using the density-functional perturbation theory. It seems that Co_2MnAl and Co_2MnGa compounds are less adequate than the Co_2MnSi and Co_2MnGe alloys for realistic spintronic applications.

References

[1] I. Galanakis, P.H. Dederichs (Eds.), Lecture Notes in Physics, vol. 676, Springer, Berlin, Heidelberg, 2005.
[2] I. Galanakis, G.A. Dederichs, N. Papanikolaou, J. Phys. D 39 (2006) 765–775.
[3] A. Bergmann, J. Grabis, B.P. Toperverg, V. Leiner, M. Wolff, H. Zabel, K. Westerholt, Phys. Rev. B 72 (2005) 214403;
J. Grabis, A. Bergmann, A. Nefedov, K. Westerholt, H. Zabel, Phys. Rev. B 72 (2005) 024437.
[4] S. Kämmerer, A. Thomas, A. Hütten, G. Reiss, Appl. Phys. Lett. 85 (2004) 79;
J. Schmalhorst, S. Kämmerer, M. Sacher, G. Reiss, A. Hütten, A. Scholl, Phys. Rev. B 70 (2004) 024426.
[5] Y. Sakuraba, M. Hattori, M. Oogane, H. Kubota, Y. Ando, H. Kato, A. Sakuma, T. Miyazaki, Appl. Phys. Lett. 88 (2006) 192508;
Y. Sakuraba, J. Nakata, M. Oogane, Y. Ando, H. Kato, A. Sakuma, T. Miyazaki, H. Kubota, Appl. Phys. Lett. 88 (2006) 022503;
Y. Sakuraba, T. Miyakoshi, M. Oogane, H. Kubota, Y. Ando, A. Sakuma, T. Miyazaki, Appl. Phys. Lett. 89 (2006) 052508.
[6] X.Y. Dong, C. Adelmann, J.Q. Xie, C.J. Palmstrom, X. Lou, J. Strand, P.A. Crowell, J.-P. Barnes, A.K. Petford-Long, Appl. Phys. Lett. 86 (2005) 102107.
[7] R.A. de Groot, F.M. Muller, P.G. van Engen, K.H.J. Buschow, Phys. Rev. Lett. 50 (1983) 2024.
[8] J. Enkovaara, A. Ayuela, A.T. Zayak, P. Entel, L. Nordström, M. Dube, J. Jalkanen, J. Impola, R.M. Nieminen, Mater. Sci. Eng., A 378 (2004) 52–60.
[9] G.H. Fecher, C. Felser, J. Phys. D 40 (2007) 1582–1586.
[10] S. Fujii, S. Sugimura, S. Ishida, S. Asano, J. Phys.: Condens. Matter 2 (1990) 8583–8589.
[11] S. Picozzi, A. Continenza, A.J. Freeman, Phys. Rev. B 66 (2002) 094421.
[12] L. Ritchie, G. Xiao, Y. Ji, T.Y. Chen, C.L. Chien, M. Zhang, J. Chen, Z. Liu, G. Wu, X.X. Zhang, Phys. Rev. B 68 (2003) 104430.
[13] L.J. Singh, Z.H. Barber, Y. Miyoshi, Y. Bugoslavsky, W.R. Branford, L.F. Cohen, Appl. Phys. Lett. 84 (2004) 2367–2369.
[14] R. Shan, H. Sukegawa, W.H. Wang, M. Kodzuka, T. Furubayashi, T. Ohkubo, S. Mitani, K. Inomata, K. Hono, Phys. Rev. Lett. 102 (2009) 246601.
[15] S. Wurmehl, G.H. Fecher, H.C. Kandpal, V. Ksenofontov, C. Felser, H.-J. Lin, J. Morais, Phys. Rev. B 72 (2005) 184434.
[16] I. Galanakis, P.H. Dederichs, N. Papanikolaou, Phys. Rev. B 66 (2002) 174429.
[17] J. Kübler, G.H. Fecher, C. Felser, Phys. Rev. B 76 (2007) 024414.
[18] B. Balke, G.H. Fecher, H.C. Kandpal, C. Felser, K. Kobayashi, E. Ikenaga, J.-J. Kim, S. Ueda, Phys. Rev. B 74 (2006) 104405.
[19] G.H. Fecher, H.C. Kandpal, S. Wurmehl, C. Felser, G. Schönhense, J. Appl. Phys. 99 (2006) 08J106.
[20] J. Kübler, Physica B 127 (1984) 257–263.
[21] S. Ishida, S. Fujii, S. Kashiwagi, S. Asano, J. Phys. Soc. Jpn. 64 (1995) 2152–2157.
[22] S. Ishida, T. Masaki, S. Fujii, S. Asano, Physica B 245 (1998) 1–8.
[23] P.M. Tedrow, R. Meservey, Phys. Rev. B 7 (1973) 318–326.
[24] R.J. Soulen Jr., J.M. Byers, M.S. Osofsky, B. Nadgorny, T. Ambrose, S.F. Cheng, P.R. Broussard, C.T. Tanaka, J. Nowak, J.S. Moodera, A. Barry, J.M.D. Coey, Science 282 (1998) 85–88.
[25] H.C. Kandpal, G.H. Fecher, C. Felser, G. Schönhense, Phys. Rev. B 73 (2006) 094422.
[26] P.J. Webster, J. Phys. Chem. Solids 32 (1971) 1221–1231.
[27] P.J. Brown, K.U. Neumann, P.J. Webster, K.R.A. Ziebeck, J. Phys.: Condens. Matter 12 (2000) 1827–1835.
[28] M.P. Raphael, B. Ravel, M.A. Willard, S.F. Cheng, B.N. Das, R.M. Stroud, K.M. Bussmann, J.H. Claassen, V.G. Harris, Appl. Phys. Lett. 79 (2001) 4396–4398.
[29] E. Şaşıoğlu, L.M. Sandratskii, P. Bruno, I. Galanakis, Phys. Rev. B 72 (2005) 184415.
[30] D. Vanderbilt, Phys. Rev. B 41 (1990) 7892–7895.
[31] J.P. Perdew, K. Burke, M. Ernzerhof, Phys. Rev. Lett. 77 (1996) 3865–3868.
[32] J.P. Perdew, K. Burke, M. Ernzerhof, Phys. Rev. Lett. 78 (1996) 1396.
[33] P. Giannozzi, S. Baroni, N. Bonini, M. Calandra, R. Car, C. Cavazzoni, D. Ceresoli, G.L. Chiarotti, M. Cococcioni, I. Dabo, A. Dal Corso, S. Fabris, G. Fratesi, S. de Gironcoli, R. Gebauer, U. Gerstmann, C. Gougoussis, A. Kokalj, M. Lazzeri, L. Martin-Samos, N. Marzari, F. Mauri, R. Mazzarello, S. Paolini, A. Pasquarello, L. Paulatto, C. Sbraccia, S. Scandolo, G. Sclauzero, A.P. Seitsonen, A. Smogunov, P. Umari, R.M. Wentzcovitch, J Phys.: Condens. Matter 21 (2009) 395502.
[34] M. Methfessel, A.T. Paxton, Phys. Rev. B 40 (1989) 3616–3621.
[35] S. Baroni, P. Giannozzi, A. Testa, Phys. Rev. Lett. 58 (1987) 1861–1864.
[36] J. Kübler, A.R. Williams, C.B. Sommers, Phys. Rev. B 28 (1983) 1745.
[37] F.D. Murnaghan, Proc. Natl. Acad. Sci. USA 50 (1944) 697.
[38] H.C. Kandpal, G.H. Fecher, C. Felser, J. Phys. D 40 (2007) 1507–1523.
[39] M. Sargolzaei, M. Richter, K. Koepernik, I. Opahle, H. Eschrig, I. Chaplygin, Phys. Rev. B 74 (2006) 224410.
[40] G. Gökoğlu, O. Gülseren, Eur. Phys. J. B 76 (2010) 321–326.
[41] A. Ayuela, J. Enkovaara, K. Ullakko, R.M. Nieminen, J. Phys.: Condens. Matter 11 (1999) 2017–2026.
[42] A.T. Zayak, P. Entel, K.M. Rabe, W.A. Adeagbo, M. Acet, Phys. Rev. B 72 (2005) 054113.
[43] M.E. Fine, L.D. Brown, H.L. Marcus, Scripta Met. 18 (1984) 951–956.
[44] S.Q. Wang, H.Q. Ye, Phys. Stat. Sol. B 240 (2003) 45–54.
[45] X.-Q. Chen, R. Podloucky, P. Rogl, J. Appl. Phys. 100 (2006) 113901.
[46] M. Born, K. Huang, Dynamical Theory of Crystal Lattices, Clarendon, Oxford, 1954.
[47] V. Jung, G.H. Fecher, B. Balke, V. Ksenofontov, C. Felser, J. Phys. D: Appl. Phys. 42 (2009) 084007.
[48] L. Chioncel, E. Arrigoni, M.I. Katsnelson, A.I. Lichtenstein, Phys. Rev. Lett. 96 (2006) 137203.